Archives of Mechanics • Archiwum Mechaniki Stosowanej • 30, 6, pp. 757–768, Warszawa 1978

Exact stability analysis of uniform cantilevered pipes conveying fluid or gas

M. BECKER (WUPPERTAL), W. HAUGER (HAMBURG)
and W WINZEN (PFORZHEIM)

A COMPLETE exact stability analysis of uniform cantilevered pipes conveying fluid or gas is given which does not require the assumption of sufficiently small velocity-dependent forces. The critical loads, the critical frequencies and the corresponding mode shapes are determined and the results are verified experimentally. The investigation includes cantilevered pipes resting on several types of elastic foundations. The influence of the various system parameters, including internal as well as external damping forces, is established.

Podano pełną ścisłą analizę stateczności rur wysięgnikowych o stałym przekroju przenoszących ciecz lub gaz, bez wprowadzania założenia o wystarczająco małych siłach zależnych od prędkości. Określono obciążenia krytyczne, krytyczne częstości i odpowiadające im postacie drgań, a wyniki sprawdzono doświadczalnie. W badaniach rozważano rury wysięgnikowe leżące na kilku typach podłoża sprężystego. Wykazano wpływ różnych parametrów układu z wewnętrznymi i zewnętrznymi siłami tłumiania włącznie.

Приведен полный точный анализ устойчивости равномерных стрелочных труб переносящих жидкость или газ без ввода предположения о достаточно малых силах зависящих от скорости. Определены критические нагрузки, критические частоты и отвечающие им типы колебаний, а результаты проверены экспериментально. В исследованиях рассмотрены стрелочные трубы, находящиеся на нескольких типах упругого основания. Показано влияние разных параметров системы с внутренними и внешними силами затухания включительно.

List of notations

b_1 damping coefficient of the Winkler foundation,
b_2 damping coefficient of the rotatory foundation,
b_3 viscous modulus,
C_j constants of integration,
c_1 modulus of the Winkler foundation,
c_2 modulus of the rotatory foundation,
E Young's modulus,
I moment of inertia,
i imaginary unit,
l length of the pipe,
P conservative end load,
P_c critical value of P,
P_{exp} experimental value of P_c,
r real part of the eigenvalue Ω,
s imaginary part of the eigenvalue Ω,
t time,
v constant velocity of the fluid,

w transverse deflection of the pipe,
x coordinate along the axis of the pipe,
y function of the mode shape,
α flexural rigidity,
β_1 dimensionless damping coefficient of the Winkler foundation,
β_2 dimensionless damping coefficient of the rotatory foundation,
β_3 dimensionless viscous modulus,
$\varkappa_1$ dimensionless modulus of the Winkler foundation,
$\varkappa_2$ dimensionless modulus of the rotatory foundation,
λ_j roots of the characteristic equation,
μ ratio of critical loads,
ξ dimensionless coordinate along the axis of the pipe,
ϱ mass of the fluid and pipe per unit length,
ϱ_F mass of the fluid per unit length,
ϱ_P mass of the pipe per unit length,
φ dimensionless load parameter,
φ_c critical value of φ,
φ_{exp} experimental value of φ_c,
ω frequency of the vibration,
Ω dimensionless frequency of the vibration.

1. Introduction

THE DYNAMIC behaviour of pipes containing flowing fluid or gas is of interest for numerous practical applications and thus has been the subject of investigations for many years (see, for example [1–3]). In particular, ROTH [4] and NEMAT-NASSER, PRASAD and HERRMANN [5] determined at about the same time flutter loads of fluid conveying cantilevered pipes, using approximate methods.

In the present paper, a complete exact analysis of the stability of uniform cantilevered pipes conveying fluid or gas, respectively, is given. In contrast to the method in [5], the analysis does not require the assumption of sufficiently small velocity-dependent forces. In addition to the critical loads, the critical frequencies as well as the corresponding mode shapes are determined. The dynamic behaviour of the pipes for load parameters below or above the critical values can also be described. Moreover, the theoretical results are verified by experiments.

The investigation includes cantilevered pipes resting on an elastic foundation. Three distinct types of foundation are considered, namely, a Winkler-type foundation, a rotatory foundation which causes restoring moments proportional to the slope of the pipe, and a generalized foundation. External damping of the foundation as well as internal damping of the pipe are also taken into account.

2. Eigenvalue problem and stability analysis

We consider a slender cantilevered pipe of the length l, constant moment of inertia I and constant mass density ϱ_p, Fig. 1. The material of the pipe is supposed to be viscoelastic of the Kelvin-Voigt type. Let E be Young's modulus, b_3 the viscous modulus and $\alpha = EI$ the flexural rigidity of the undamped pipe. The pipe contains an incompressible

fluid or an ideal gas, respectively, which is flowing at a constant velocity v. The mass per unit length of the flowing fluid or gas is denoted by ϱ_F. The flow is assumed to be uniaxial, frictionless and isothermal. The pipe is resting either on an elastic Winkler-type foundation with the constant modulus c_1 and damping coefficient b_1, on a rotatory foundation with the constant modulus c_2 and damping coefficient b_2, or on a generalized foundation, where the restoring forces and the restoring moments are acting simultaneously. It can be shown

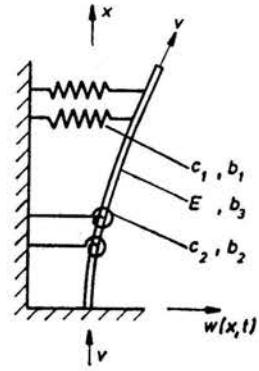

FIG. 1. Cantilevered pipe.

[6] that this generalized foundation corresponds to a Pasternak-type foundation if the modulus c_2 is taken to be equal to the shear modulus G of the foundation material.

The equation of motion for small transverse vibrations is found to be

$$b_3 I\frac{\partial^5 w}{\partial x^4\partial t}+\alpha\frac{\partial^4 w}{\partial x^4}-b_2\frac{\partial^3 w}{\partial x^2\partial t}+(\varrho_F v^2-c_2)\frac{\partial^2 w}{\partial x^2}+2\varrho_F v\frac{\partial^2 w}{\partial x\partial t}+(\varrho_P+\varrho_F)\frac{\partial^2 w}{\partial t^2}+b_1\frac{\partial w}{\partial t}+c_1 w=0, \tag{2.1}$$

and the boundary conditions are

$$w(0,t)=\frac{\partial w(0,t)}{\partial x}=0,$$

$$b_3 I\frac{\partial^3 w(l,t)}{\partial x^2\partial t}+\alpha\frac{\partial^2 w(l,t)}{\partial x^2}=0, \tag{2.2}$$

$$b_3 I\frac{\partial^4 w(l,t)}{\partial x^3\partial t}+\alpha\frac{\partial^3 w(l,t)}{\partial x^3}-b_2\frac{\partial^2 w(l,t)}{\partial x\partial t}-c_2\frac{\partial w(l,t)}{\partial x}=0.$$

It should be noted that the boundary conditions contain the foundation coefficient c_2 as well as the damping coefficients b_2 and b_3 [7] which is an intuitively unexpected feature.

Upon stipulation of

$$w(x,t)=e^{i\omega t}y(x),\quad i=\sqrt{-1}, \tag{2.3}$$

one obtains the non-self-adjoint eigenvalue problem

$$(1+i\Omega\beta_3)y^{IV}+(\phi-\varkappa_2-i\Omega\beta_2)y''+2i\Omega\sqrt{\phi}\sqrt{\varrho_F/\varrho}y'+(\varkappa_1+i\Omega\beta_1-\Omega^2)y=0, \tag{2.4}$$

$$y(0)=y'(0)=y''(1)=0,$$

$$(1+i\Omega\beta_3)y'''(1)-(\varkappa_2+i\Omega\beta_2)y'(1)=0, \tag{2.5}$$

where

$$\begin{aligned} &\phi = \varrho_F v^2 l^2/\alpha, \quad \Omega = \sqrt{\varrho}\omega l^2/\sqrt{\alpha}, \\ &\varkappa_1 = c_1 l^4/\alpha, \quad \varkappa_2 = c_2 l^2/\alpha, \\ &\beta_1 = b_1 l^2/\sqrt{\alpha\varrho}, \quad \beta_2 = b_2/\sqrt{\alpha\varrho}, \quad \beta_3 = b_3 I/(l^2\sqrt{\alpha\varrho}), \\ &\varrho = \varrho_P + \varrho_F, \end{aligned} \tag{2.6}$$

and the primes indicate derivatives with respect to the dimensionless coordinate $\xi = x/l$. The quantity ϱ_F/ϱ satisfies the condition

$$0 < \varrho_F/\varrho < 1. \tag{2.7}$$

A solution of the differential equation (2.4) is given by

$$y(\xi) = \sum_{j=1}^{4} C_j e^{i\lambda j \xi}, \tag{2.8}$$

where $\lambda_j, j = 1, 2, 3, 4$ are the four roots of the characteristic equation

$$(1+i\Omega\beta_3)\lambda^4 - (\phi - \varkappa_2 - i\Omega\beta_2)\lambda^2 - 2\Omega\sqrt{\phi}\sqrt{\varrho_F/\varrho}\lambda + (\varkappa_1 + i\Omega\beta_1 - \Omega^2) = 0 \tag{2.9}$$

and the C_j are constants of integration. Unfortunately, the characteristic equation (2.9) is not a biquadratic equation as in [7] or in the case of Beck's column [8]. Accordingly, the analysis is far more complicated than it was there. Upon introduction of Eq. (2.8) and the appropriate derivatives into the boundary conditions (2.5), one obtains the system of linear homogeneous equations for the constants C_j

$$\begin{aligned} &\sum_{j=1}^{4} C_j = 0, \\ &\sum_{j=1}^{4} \lambda_j C_j = 0, \\ &\sum_{j=1}^{4} \lambda_j^2 e^{i\lambda_j} C_j = 0, \\ &\sum_{j=1}^{4} [-i\lambda_j^3(1+ui\Omega\beta_3) - i\varkappa_2\lambda_j + \Omega\beta_2\lambda_j] e^{i\lambda_j} C_j = 0. \end{aligned} \tag{2.10}$$

A necessary and sufficient condition for the existence of a non-trivial solution is that the determinant of the coefficients vanishes which leads, after some calculation, to a complicated eigenvalue equation of the form

$$D(\lambda_j, \varkappa_2, \beta_2, \beta_3, \Omega) = 0. \tag{2.11}$$

The eigenvalue equation (2.11) yields in general complex eigenvalues

$$\Omega = r + is. \tag{2.12}$$

Equations (2.3), (2.6) and

$$e^{i\omega t} = e^{i\sqrt{\alpha}/(l^2\sqrt{\varrho})rt} e^{-\sqrt{\alpha}/(l^2\sqrt{\varrho})st} \tag{2.13}$$

show that the dynamic behaviour of the pipe is governed by the imaginary parts of the eigenvalues Ω. For $s > 0$ one has a damped vibration, $s = 0$ corresponds to a steady state motion, and $s < 0$ leads to an exponentially growing unbounded solution of the differential

equation (2.1). Thus the critical value of the dimensionless load parameter ϕ is given by the condition $s = 0$.

It is quite cumbersome to determine numerically the complex eigenvalues Ω which depend, for given values of the other quantities, on the parameter ϕ. However, the complex analysis has the advantage that it supplies, in addition to the critical value ϕ_c, information about the dynamic behaviour of the pipe for load parameters ϕ below or above the critical value.

3. Examples

3.1. Undamped pipe without foundation

As a first example, we consider an undamped pipe without foundation, i.e. $\varkappa_1 = \varkappa_2 = \beta_1 = \beta_2 = \beta_3 = 0$. For Beck's column [8], the eigenvalue curve "load vs. frequency" can be illustrated in the real frequency-load-plane. As a consequence of the complex eigen-

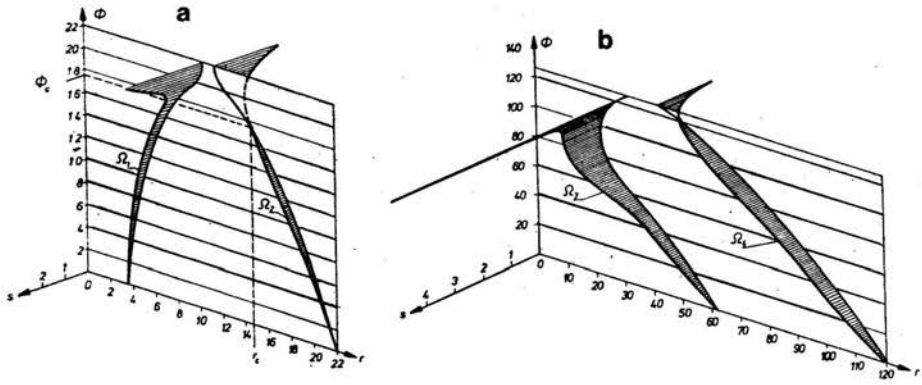

FIG. 2. Spatial eigenvalue curves.

values Ω for the fluid or gas conveying pipe, we need a spatial representation as shown in Figs. 2a and 2b, where the eigenvalue curves $\phi = \phi(\Omega)$ for the first four eigenvalues $\Omega_1, \ldots, \Omega_4$ are given. The ratio of the mass densities appearing in Eq. (2.7) is taken as

$$\varrho_F/\varrho = 10^{-3}.$$

A slight variation of this value does not change the eigenvalue curves qualitatively, and thus does not alter the conclusions drawn below.

Figures 2a and 2b give a very clear description of the character of the eigenvalue curves. One can easily see that for small values of ϕ all four curves are in the half-space $s > 0$ which corresponds to a damped vibration of the pipe and hence to stability. For increasing velocity of the flowing medium, that is for increasing values of ϕ, the imaginary parts of the first and the third curve increase, too, whereas the second and the fourth curve intersect the r, ϕ-plane and continue into the unstable half-space $s < 0$. Hence the stability is not lost, as one might expect, on the first branch of the eigenvalue curves (which corresponds to the first eigenvalue), but it is lost on the second branch. The critical value of the load parameter and the corresponding value of the frequency are

$$\phi_C = 17.6, \quad \Omega_C = 14.6, \tag{3.1}$$

according to Fig. 2a. It is noted that for $\varrho_F/\varrho = 10^{-2}$ the curves are similar and

$$\phi_C = 17.96. \tag{3.2}$$

This value will be needed later.

In the following, two projections of the spatial eigenvalue curves into the r, ϕ-plane and into the s, ϕ-plane will be used for simplicity. The projections of the first two branches

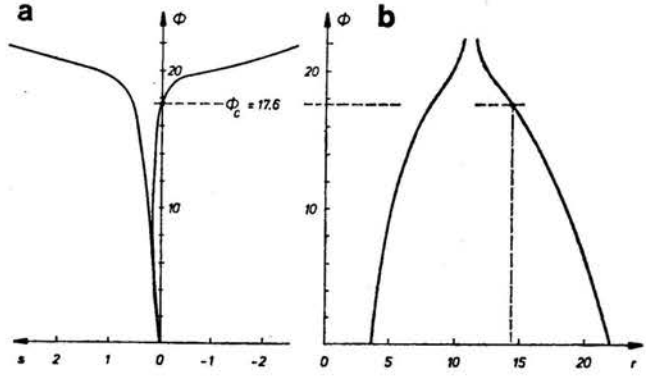

FIG. 3. Projections of the eigenvalue curves.

are given in Figs. 3a and 3b. They show very clearly the critical load on the second branch, and the imaginary parts s allow to draw immediate conclusions on the dynamic behaviour of the pipe for arbitrary values of the load ϕ.

Since the critical load is found to be on the second branch, the unstable motion of the pipe for $\phi > \phi_C$ has to correspond to the second mode shape of the pipe instead of the

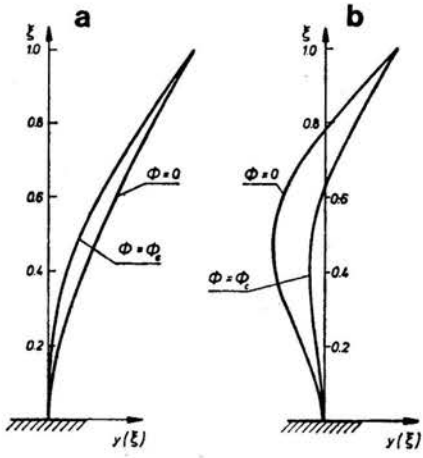

FIG. 4. Mode shapes.

first one. The first two mode shapes were determined numerically and are displayed in Figs. 4a and 4b for $\phi = 0$ and $\phi = \phi_C$, respectively. One can see that the nodal point of the second mode shape is shifted from $\xi = 0.78$ for $\phi = 0$ to $\xi = 0.63$ for $\phi = \phi_C$. The unstable vibration which is initiated at $\phi = \phi_C$ has to occur in the latter form. This is verified by the experiments described below.

3.2. Experimental investigation

It is one of the objectives of this study to design an experimental setup as simple as possible in order to verify the theoretical results obtained above. First of all, it appears to be much simpler to use air instead of water as the flowing medium. This choice, however, leads to the requirement of a relatively small flexural rigidity of the pipe in order to have instability at an obtainable velocity of the flow. After several preliminary tests with various pipes, it turned out that plastic drinking straws are very well suited for the experiments.

The pipes used in the tests are between 10 cm and 26 cm long, the internal diameter is approximately 0.31 cm and the external diameter 0.33 cm. In order to avoid the difficulties which are involved in a sufficiently accurate determination of the flexural rigidity of the pipe, an indirect way to obtain the critical load is used. This method compares the critical load of the present problem with the critical load of a well-known conservative problem and it has the advantage that the unknown flexural rigidity is eliminated.

In a first experiment, the pipe is pinned at both ends and loaded only with a conservative end load P. According to Euler, the (theoretical) critical value of the load is

$$P_C = \pi^2 \alpha / l^2. \tag{3.3}$$

The pipe is connected to weighing scales which allow to measure the reaction force and hence the critical load as well to an accuracy of $0.2 \cdot 10^{-2}$ N. The critical load thus obtained experimentally is denoted by P_{exp}.

In a second experiment, the pipe is clamped at the base and free at the other end. The base is again fixed to weighing scales and the pipe is connected to a central supply of pressurized air with a maximum available pressure of 60 N/cm^2. The pressure of the air (and thus the velocity of the flow) is gradually increased until the stability boundary is reached. The scales then give a load corresponding to the critical value ϕ_{exp}.

Let

$$\mu_C = \phi_C/(P_C l^2/\alpha), \quad \mu_{exp} = \phi_{exp}/(P_{exp} l^2/\alpha) \tag{3.4}$$

be the ratios of the theoretical or experimental values, respectively, of the critical loads of the non-conservative problem (pipe) and the conservative problem (Euler). The ratio of the mass densities in the experiments is $\varrho_F/\varrho \approx 10^{-2}$. Thus from Eqs. (3.2) and (3.3) we obtain the following theoretical value:

$$\mu_C = 1.82. \tag{3.5}$$

Performing the experiments described above with various pipes one then has

$$\mu_{exp} = 2.01. \tag{3.6}$$

By comparison, one obtains

$$\phi_{exp} = \phi_C \mu_{exp}/\mu_C = 19.8. \tag{3.7}$$

This value is about 10% larger than the theoretical value, Eq. (3.2). However, considering on one hand the simplicity of the experimental setup (which does not require any sophisticated equipment at all), and on the other hand the simplicity of the theory (where important effects such as damping are neglected), this is quite a good agreement. It might be mentioned that the critical velocity of the flow is of the order of 150 m/sec.

With the aid of a stroboscope one can measure the frequency of the vibration at the stability boundary. In addition, photographs of the unstable oscillation confirm the theoretical prediction that instability has to occur in the second mode. The mode shape

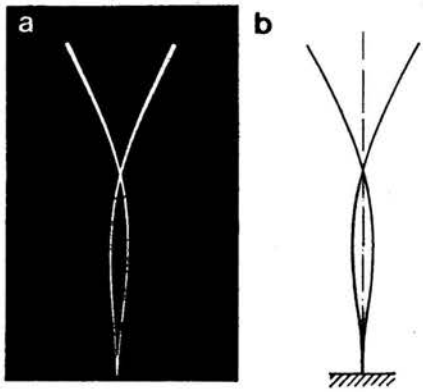

FIG. 5. Comparison of experimental and theoretical mode shapes.

taken from a photograph and the theoretical mode shape according to Fig. 4b are compared in Figs. 5a and 5b and they show excellent agreement.

It was found in Sect. 3.1 that for increasing velocity of the flowing medium the imaginary part s of the first branch of the eigenvalue curve increases, see Fig. 3a. Thus the damping of the first mode increases with increasing velocity. This fact can easily be observed experimentally if free vibrations of the loaded pipe in the first mode are considered.

3.3. Pipe on a Winkler foundation

We consider now a pipe resting on a Winkler foundation, i.e. $\varkappa_2 = \beta_2 = 0$. The results of the numerical analysis for $\varrho_F/\varrho = 10^{-3}$ are displayed for several values of the foundation modulus $\varkappa_1$, the damping coefficient β_1 of the foundation and the coefficient β_3 of the internal damping in Figs. 6a and 6b. In Fig. 6a, only those curves which intersect the ϕ-axis are given.

In comparison with Figs. 3a and 3b one can see that the foundation changes the eigenvalue curves considerably. One can easily show from Eq. (2.9) that for $\beta_3 = 0$ and $\phi = 0$ the eigenvalues Ω are given by

$$\Omega = \Omega_0 \sqrt{1 + \frac{\varkappa_1}{\Omega_0^2} - \frac{\beta_1^2}{4\Omega_0^2}} + \frac{1}{2} i\beta_1, \tag{3.8}$$

where Ω_0 are the eigenfrequencies of a free, unloaded cantilever.

Thus, if no damping is present ($\beta_1 = 0$), the eigenvalues Ω have no imaginary parts for $\phi = 0$ and the points of the eigenvalue curve are only shifted along the r-axis with an increasing foundation modulus. For example, the initial point of the first branch is shifted from $\Omega = \Omega_0 = 3.516$ for $\varkappa_1 = 0$, see Fig. 3b, to $\Omega = 4.73$ for $\varkappa_1 = 10$ or to $\Omega = 7.90$ for $\varkappa_1 = 50$, see Fig. 6b. In the undamped case, the numerical analysis does not give imag-

inary parts of Ω for $\phi \neq 0$ either, and the critical load is given by the point with a horizontal tangent of the curve $\phi = \phi(r)$. Figure 6b indicates that

$$\phi_C = 19.36 \quad \text{for} \quad \varkappa_1 = 10 \quad \text{and} \quad \phi_C = 19.32 \quad \text{for} \quad \varkappa_1 = 50. \tag{3.9}$$

Hence, by comparison with Eq. (3.1), it is noticed that the Winkler foundation has a stabilizing effect on the pipe. This contrasts with the non-existing effect of a Winkler founda-

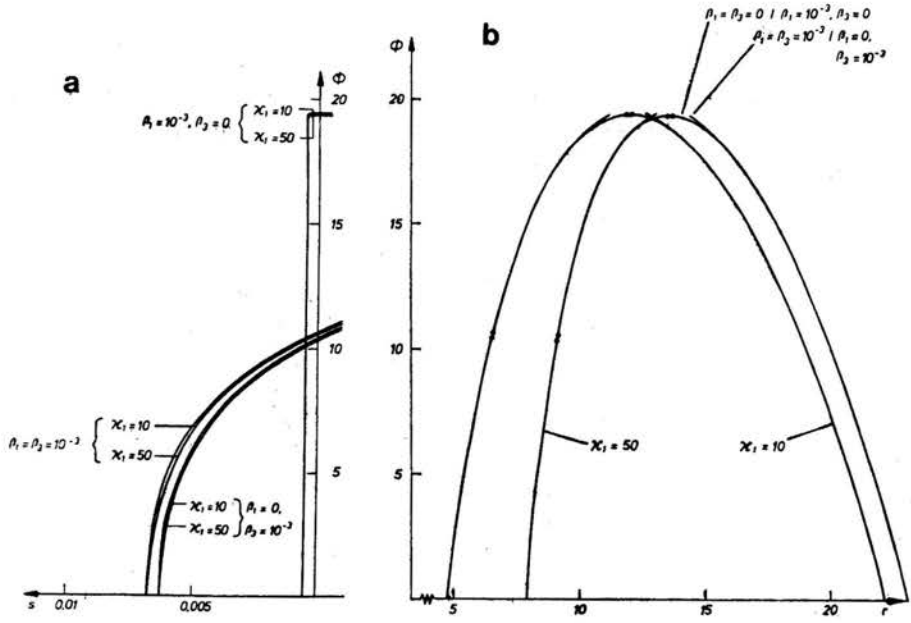

FIG. 6. Eigenvalue curves for a pipe on a Winkler foundation.

tion on the stability of Beck's column [9]. An increasing foundation modulus may surprisingly decrease the stability again, see Eq. (3.9), however, this effect does not appear to be very strong.

If one includes damping of the foundation, the eigenvalues Ω have the imaginary part $s = \frac{1}{2}\beta_1$ for $\phi = 0$ according to Eq. (3.8). Figure 6a shows that this value remains practically unchanged up to loads ϕ just below the critical value. The influence of the damping on the flutter load (slightly destabilizing) is practically not noticeable and ϕ_C is again given by Eq. (3.9). The damping, however, causes a slight increase of the corresponding critical value r_C and the critical point (r_C, ϕ_C) is thus shifted to the right of the maximum of the curve $\phi = \phi(r)$. This implies that the stability is lost again on the second branch of the eigenvalue curves.

Finally, we also include internal damping of the pipe. Figure 6a shows that for $\beta_3 \neq 0$ the critical load is considerably reduced. For example, one obtains $\phi_C = 10.69$ for $\varkappa_1 = 10$ and $\beta_3 = 10^{-3}$ as compared to $\phi_C = 19.36$ for $\varkappa_1 = 10$ and $\beta_3 = 0$. It is remarkable that

the stability is lost now on the first branch of the eigenvalue curves. An increasing foundation modulus again has a destabilizing influence which, however, is more pronounced than in the undamped case. Damping of the foundation now has a noticeable stabilizing effect in contrast to the result found above. This is easily explained by the fact that viscous damping of the foundation causes an increase of the critical frequency which, on the first branch of the eigenvalue curves, results in an increase of the critical load.

3.4. Pipe on a rotatory foundation

Consider now a pipe resting on a rotatory foundation. Then $\varkappa_1 = \beta_1 = 0$. The results of the numerical analysis are shown for $\varrho_F/\varrho = 10^{-3}$ in Figs. 7a and 7b. The critical load in the completely undamped case is again given by the maximum of the curve $\phi = \phi(r)$.

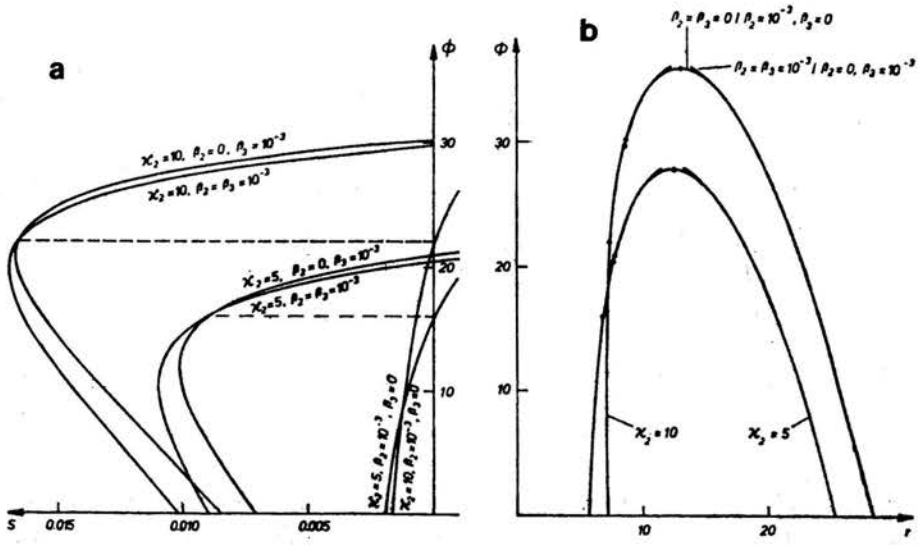

FIG. 7. Eigenvalue curves for a pipe on a rotatory foundation.

One can see that the foundation has a strong stabilizing effect which increases with the increasing foundation modulus $\varkappa_2$. This is in contrast to the result obtained for a Winkler foundation. Also in contrast to the results found above, the damping of the foundation now has a considerable destabilizing influence, whereas the inclusion of internal damping of the pipe increases the stability. In addition, viscous damping of the rotatory foundation decreases the critical frequency and thus the stability of the pipe even in the presence of internal damping.

A further remark should be made. Consider the two curves for $\varkappa_2 = 10$, $\beta_3 = 10^{-3}$, and $\beta_2 = 0$ or $\beta_2 = 10^{-3}$, respectively, in Fig. 7a. It is observed that these two curves intersect at the critical value ϕ_C of the system with the parameters $\varkappa_2 = 10$, $\beta_2 = 10^{-3}$ and $\beta_3 = 0$ (which can be interpreted as the point of intersection of the two curves for

$\varkappa_2 = 10$, $\beta_3 = 0$, and $\beta_2 = 0$ or $\beta_2 = 10^{-3}$, respectively). The same result is also obtained for other values of the system parameters as indicated by the dashed lines in Fig. 7a. A similar feature has already been noticed in the case of Beck's column on a rotatory foundation [7]. No physical significance could be associated with this phenomenon.

3.5. Pipe on a generalized foundation

Finally, we study the stability of a pipe resting on a generalized foundation where the restoring forces and the restoring moments are acting simultaneously. The parameters used are $\varrho_F/\varrho = 10^{-3}$, $\varkappa_1 = 50$ and $\varkappa_2 = 5$. Figures 8a and 8b show that the stability behaviour is essentially like that of a pipe on a rotatory foundation.

In the completely undamped case, the critical load is given as before by the maximum of the curve $\phi = \phi(r)$. One obtains $\phi_C = 27.81$ as compared to $\phi_C = 27.89$ for the pipe

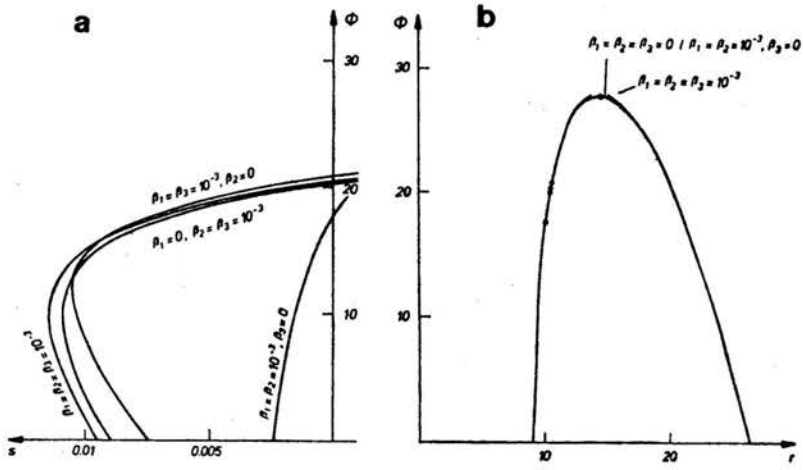

FIG. 8. Eigenvalue curves for a pipe on a generalized foundation

on a rotatory foundation with the same value of the modulus $\varkappa_2$. Hence the restoring forces, i.e. the Winkler part of the foundation, unexpectedly reduce the stability of the pipe. Small damping of the foundation has a strong destabilizing effect, whereas internal damping of the pipe increases the stability again. However, the critical value of the load is still less than the one for the completely undamped system. As for the pipe on a rotatory foundation, all the crictical points are found on the first branch of the eigenvalue curves.

References

1. H. ASHLEY and G. HAVILAND, *Bending vibrations of a pipe line containing flowing fluid*, J. Appl. Mech., 17, 229–232, 1950.
2. R. W. GREGORY and M. P. PAIDOUSSIS, *Unstable oscillations of tubular cantilevers conveying fluid*, Proc. Roy. Soc. London, 293, 512–542, 1966.

3. R. E. D. BISHOP and I. FAWZY, *Free and forced oscillation of a vertical tube containing flowing fluid*, Proc. Roy. Soc. London, 284, 1–47, 1976.
4. W. ROTH, *Instabilität des durchströmten, einseitig eingespannten Rohres*, Oelhydr. und Pneumat., 10, 58–64, 1966.
5. S. NEMAT-NASSER, S. N. PRASAD and G. HERRMANN, *Destabilizing effect of velocity-dependent forces in nonconservative continuous systems*, AIAA Journal, 4, 1276–1280, 1966.
6. A. D. KERR, *Elastic and viscoelastic foundation models*, J. Appl. Mech., 31, 491–498, 1964.
7. M. BECKER, W. HAUGER and W. WINZEN, *Influence of internal and external damping on the stability of Beck's column on an elastic foundation*, J. Sound Vibr., 54, 468–472, 1977.
8. M. BECK, *Die Knicklast des einseitig eingespannten, tangential gedrückten Stabes*, ZAMP, 3, 225–228, 1952. Errata: ZAMP, 3, 476–477, 1952.
9. T. E. SMITH and G. HERRMANN, *Stability of a beam on an elastic foundation subjected to a follower force*, J. Appl. Mech. 39, 628–629, 1972.

GESAMTHOCHSCHULE WUPPERTAL
WUPPERTAL, WEST GERMANY,

HOCHSCHULE DER BUNDESWEHR HAMBURG
HAMBURG, WEST GERMANY

and

METALLSCHLAUCH-FABRIK PFORZHEIM
PFORZHEIM, WEST GERMANY

Received September 8, 1977.